A comparative study of the rheological properties of three different nanofibrillated cellulose systems

Ali Naderi and Tom Lindström

KEYWORDS: Nanofibrillated cellulose; Rheology; Wall-slip effects; Temperature; Ionic strength; thixotropy.

SUMMARY: The rheological properties of NFC systems in different conditions are of important for their handling and implementation in various industrial applications. In this investigation, the existence of wall-slip effects and the rheological characteristics of three different nano-fibrillated cellulose (NFC) systems - enzymatically pre-treated (NFC_{Enz}), carboxymethyl cellulose grafted (NFC_{CMC}) and carboxymethylated (NFC_{Carb}) - were investigated.

It was found that the rheological properties of NFC_{Carb} are less affected by wall-slip effects when geometries with serrated surfaces are employed. The other systems showed, however, different degrees of susceptibility to these effects. The thixotropic properties of the different NFC systems, together with the impact of ambient ionic strength and temperature on the rheological properties of the systems, were also studied. It was found that the different systems displayed different rheological behaviours. In short, all systems regained most of their original properties as soon as severe shearing was ceased. The apparent viscosities of NFC_{Enz} and NFC_{CMC} were found to be little affected by the ionic strength of the system. However, the viscosity of the systems decreased somewhat with increasing temperatures. The viscosity of NFC_{Carb} decreased on the other hand with the increasing ionic strength, but otherwise showed little sensitivity towards the ambient temperature. Hence, it was concluded that the rheological properties of NFC_{Carb} were primarily governed by the electrosteric interactions between the NFC entities rather than the viscous properties of the liquid phase.

ADDRESSES OF THE AUTHORS: Ali Naderi (ali.naderi@innventia.com), **Tom Lindström** (tom.lindstrom@innventia.com)
Innventia AB, Box 5604 SE-114 86 Stockholm, Sweden.
Corresponding author: Ali Naderi

Nanofibrillated cellulose (NFC) denotes nano-sized cellulosic materials with width- and length values less than 100 nm and several micrometres, respectively (Moon et al. 2011; Isogai 2013; Lindström et al. 2014). The NFC manufacturing process often involves a chemical treatment of the cellulosic material (e.g. carboxymethylation (Walecka 1956), enzymatic treatment (Henriksson et al. 2007), CMC grafting (Laine et al. 2000) and TEMPO oxidation (Isogai et al. 2011)), followed by a mechanical delamination process, viz. high pressure homogenization, grinding, cryocrushing or any other communition treatment. Understandably, the multitude of the chemo-mechanical processes and their combinations lead to different properties with respect to morphology and surface properties. For example, enzymatically pre-treated NFC systems are characterized by close-to-uncharged bundles of nanofibrils (width < 100 nm), exhibiting a broad size distribution. On the other hand, TEMPO-based or carboxymethylated NFC systems are highly charged systems, exhibiting a much narrower size distribution. The measured widths of the NFC strands of these systems have been reported to range from 3-20 nm (Wågberg et al. 2008; Isogai et al. 2011).

Rheological characterization of NFC-based systems is understandably complicated by the diverse characteristics of the different NFC systems, which requires the development of different measuring protocols. For example, the authors employed pre-shearing of the samples in the analysis of a CMC-grafted NFC system (Naderi et al. 2015c) with phase-separation tendencies. A similar protocol was also found to be necessary in the study of an enzymatically pre-treated NFC (Naderi, Lindström 2015), which is also an unstable system; otherwise erroneous results would have been obtained. On the other hand, pre-shearing of samples was not viewed as necessary when the same authors investigated a highly charged carboxymethylated NFC (Naderi et al. 2014), which displayed a high colloidal stability.

Rheological measurements are further complicated by the fact that the recorded rheological properties obtained by standard rotational viscometers are the net result of all the inter-particle and particle-measuring chamber interactions. The results are hence apparent, which may have ramifications on the analysis of the results. Hence, it is necessary to combine rheological measurements with other methodologies, something that is often difficult, due to instrumental limitations. It is noted, though, that contributions exist which have addressed this inadequacy. However, the value of the approaches remains to be independently verified. For example, (Nechyporchuk et al. 2014) combined rotational viscometry measurements with camera recordings. The authors observed that a cone-plate geometry with roughened surfaces (when compared with a geometry with smooth surfaces) diminished wall-slip effects and flow instabilities. The investigations further revealed the existence of shear-banding phenomena in certain shearing conditions. However, the importance of flow instabilities and shear banding in the interpretation of the recorded rheological properties was not obvious from authors' report. On the other hand, (Karppinen et al. 2012) combined a rotational viscometry (employing a bob and cup geometry - with the latter being produced in a transparent material) with photography to investigate a commercial, low-charged NFC system. The authors reported changes in the NFC floc structure when altering the shear rate. However, the importance of the observations is ambiguous considering the macro-size of the flocs (contrasting with the nano size of NFC systems) and the afore-mentioned wall-slip effects.

As touched upon, wall-slip (also known as wall depletion) effects constitute another major challenge in the study of the rheology of NFC-based systems. Slip effects occur due to the depletion of the dispersed particles from the solid boundaries (measuring-chamber walls) leaving a liquid layer that has a lower viscosity than the bulk viscosity. Slip effects are often observed for less stable systems (Buscall 2010); for example Nechyporchuk et al. (2014) reported of slip effects for a (presumably) low-charged enzymatically pre-treated NFC, but none for a highly charged TEMPO-based NFC system. The slip effects for less stable systems might, however, be reduced by "proper" shearing of the systems prior to the measurements (Kelessidis et al. 2007; Bonn, Denn 2009).

Wall depletion effects occur also more readily at smooth boundaries, which can lead to significant errors when the relative viscosity (the ratio between the viscosity of the dispersion and the liquid phase) of the suspension is high (≥ 100, (Buscall 2010)). The wall depletion effects can, however, be significantly reduced by using serrated surfaces; the scale of surface roughness should then be of the same order as the size of the dispersed particles (Buscall 2010). In this context, it is noted that a widely publicized method based on a wide-gap bucket vane viscometer was recently proposed as an attractive methodology for performing rheological measurements with no wall depletion effects (Mohtaschemi et al. 2014). However, as has been pointed out by Nechyporchuk et al. (2015) the methodology is probably most useful in the study of dilute NFC systems (which can be effectively stirred). Furthermore, the methodology of Mohtaschemi et al. was also argued to be affected by flow localization effects. It is clear that awareness of the existence and the impact of the slip effects on the rheological properties of any investigated system is important for the analysis of the measurements.

This report aims to elucidate the impact of temperature and ionic strength (altered by a monovalent salt) on the rheological properties of enzymatic pre-treated, carboxy-methylated and CMC-grafted NFC systems (that have been produced by the same amount of mechanical shearing) with the expectation of finding different properties due to the varying chemistries of the systems. The studies are further expanded by investigating the thixotropic behaviour of the systems. The results are rationalized by taking into account the impact of eventual slip effects, which are distinguished by a route that has been proposed by Kelessidis et al. (2010).

Materials and methods

Material

A commercial never-dried TCF-bleached sulfite dissolving pulp (trade name: Dissolving Plus) from a mixture of Norway spruce (60%) and Scottish pine (40%) was obtained from Domsjö Fabriker (Domsjö Mill, Sweden). The pulp has a hemicellulose content of 4.5% (w/w) (measured as solubility in 18% NaOH, R18) and a lignin content of 0.6% (w/w).

The following materials were used in the enzymatic pre-treatment process.

KH_2PO_4 and Na_2HPO_4 (GPR Rectapur) were purchased from VWR (Sweden). These chemicals constitute the phosphate buffer in the enzymatic treatment process. A mono-component endoglucanase enzyme (FiberCare®R) was obtained from Novozym A/S (Denmark). A microbiocide, 5-chloro-2-ethyl-4-isothiazolin-3-one was purchased from Nalco AB (Sweden); the material is used to suppress the bacterial growth in the fiber suspension.

The following materials were employed in the carboxymethylation pre-treatment process.

Ethanol (Rectapur) was purchased from VWR (Sweden). Monochloroacetic acid (99%), acetic acid (ACS reagent), isopropanol (ACS reagent), sodium hydroxide (NaOH, ACS reagent), sodium hydrogen carbonate ($NaHCO_3$) and methanol (ACS reagent) were purchased from Sigma Aldrich.

The below-listed materials were used in the pre-treatment process of NFC_{CMC}.

Carboxymethyl cellulose (Aquasorb A500), with a degree of substitution of 0.4 and a molecular weight of 1000 kg/mole, was obtained from Ashland Inc. (USA). Calcium chloride ($CaCl_2$, ACS reagent) was purchased from Sigma Aldrich.

All chemicals were used as received, and deionized water was used throughout the studies.

Production of NFC systems

Enzymatically pre-treated nanofibrillated cellulose (NFC_{Enz})

The manufacturing process is similar to that reported by (Naderi et al. 2015b). In brief, the (never-dried) pulp is refined prior to the enzymatic pre-treatment[1] as a means to increase the accessibility of the cell wall to the enzyme. Thereafter, after a second refining and the addition of the microbiocide[2], the pulp suspension (≈ 2% (w/w)) is passed one time through a microfluidizer (M-110EH, Microfluidics Corp., USA) at 1700 bar through two Z-shaped chambers with diameters of 200 μm and 100 μm, respectively.

It is noted that conductometric measurements as described by Katz et al. (1984) on the pre-treated pulp (in its sodium counter-ion form) revealed a charge density of about 30 μeq/g.

Carboxymethylated nanofibrillated cellulose (NFC_{Carb})

The never dried fibers were dispersed in water at 10000 revolutions using an ordinary laboratory pulper. This was conducted in smaller batches of 30 grams of fibers in two liters of water. The fibers were then exchanged to ethanol by washing the fibers in one liter of ethanol four times with a filtering step in between.

The fibers (110 grams) were then impregnated for 30 min with a solution of 10 g of monochloroacetic acid in 500 ml of isopropanol. The fibers were then added in portions to a solution of 16.2 g of NaOH in 500 ml methanol and mixed with two litres of isopropanol that

[1]The dosage, the incubation time and the temperature of the enzyme are 0.17 μl/g fiber, 50°C and 2 h, respectively.
[2]10 ml of the biocide is added to 10 kg of the pulp suspension.

had been heated just below its boiling temperature in a five-litre reaction vessel fitted with a condenser. The carboxymethylation reaction was allowed to continue for one hour.

Following the carboxymethylation step, the fibers were filtrated and washed in three steps. First, the fibers were washed with 20 l of water. Thereafter, the fibers were washed with two liters of acetic acid (0.1 M) and finally with 10 l of water. The fibers were then impregnated with two liters of $NaHCO_3$-solution (4% w/w solution) for 60 min in order to convert the carboxyl groups to their sodium form. Then, the fibers were washed with 15 l of water and drained on a Büchner funnel.

The total charge of the pulp (and hence the resulting NFC), in its sodium counterion form, was determined by means of conductometric titration to be ca 590 μeq/g (degree of substitution (D.S.) ≈ 0.1).

The pre-treated fibers (≈ 2% (w/w)) in their sodium form were microfluidized once, by using the same settings as when NFC_{Enz} was produced.

Carboxymethyl cellulose grafted nanofibrillated cellulose (NFC_{CMC})

A detailed description of the manufacturing process of NFC_{CMC} is reported in (Naderi et al. 2015c). In brief, a 0.5% (w/w) stock solution of CMC was added at a dosage of 80 mg CMC/g pulp and stirred for one hour, upon which $CaCl_2$ was added. The pulp and $CaCl_2$ concentrations were 2.5% (w/w) and 50 mM respectively. The mixture was then heated in an oil bath for two hours at 120°C, after which the excess chemicals were removed by washing the pulp with water as described above. The pulp was then ion-exchanged to its hydrogen counterion form (with acetic acid), and washed. Conductometric measurements on the modified pulp (in its sodium counter-ion form) revealed a charge density of about 160 μeq/g. The CMC-modified pulp was exchanged to its sodium counter-ion form, and was subsequently delaminated (≈ 2% (w/w)) in the same manner as NFC_{Enz} and NFC_{Carb}.

Rheological investigations

The rheological studies were conducted on samples that had been stored in a fridge (≈ 5°C) for at least three days after their manufacture, and then equilibrated overnight at room temperature.

The investigations were performed using a Kinexus stress-controlled rotational rheometer (Malvern Instruments, UK) together with the software rSpace (Malvern Instruments, UK).

Two standardized (ISO 3219/DIN 53019) metal concentric cylinder (bob and cup) geometries with serrated surfaces were used in the studies. The height and distance between the serrations were 300 μm and 1000 μm, respectively. The diameters of the two bobs were 25 and 23 mm respectively; the length of the bobs was 37.5 mm. The diameter and wall height of the cup were 27.5 and 62.5 mm, respectively. A metal concentric cylinder geometry with smooth surfaces was also employed in the studies. The diameter and length of the bob were 25 and 37.5 mm, respectively; the diameter and height of the smooth cup were the same as the serrated equivalent. Serrated bob and cups are labelled B23 and B25, where the numbers relate to the cylinder diameter; the smooth bob and cups are labelled as BS followed by the diameter of the cylinder. A working gap of 9.15 mm was employed in all measurements (irrespective of the nature of the smoothness of the geometries).

The NFC samples were sheared at 100 s^{-1} for one minute in the measuring chamber, as a mean to even out the heterogeneities, and were then left to equilibrate for two minutes before conducting the measurements.

The controlled shear rate ($\dot{\gamma}$) measurements were conducted in $\dot{\gamma}$ = 0.1-1000 s^{-1}. Integration time per measuring point was set to 30 seconds. Oscillatory strain (γ) sweep measurements were conducted in γ = 0.01-100% at 1.592 Hz.

The experimental temperature was set, if not stated otherwise, to 25°C. The samples were covered during the studies with a protective hood to minimize their drying.

Each measurement was repeated at least two times; the experimental error was in the order of 10%.

Identification of slip effects

Slip effects in highly viscous systems viz. concentrated NFC can be easily detected by performing experiments with smooth and serrated geometries, as the viscous properties that are obtained by the former geometries are (as will be shown) lower than those obtained by using serrated geometries

However, even though slip effects can be diminished by roughening the geometries (Buscall 2010), their absence cannot automatically be presumed. In this communication a method proposed by Kelessidis et al. (2010) has been employed to point to the eventual presence of slip effects in the study of different NFC systems, under different conditions. The proposed method assumes that the rheological property (viscosity) of a system that is marred with slip effects changes with the alteration of the distance between the shearing surfaces. In this communication, the width of the shearing zone was changed by using two (serrated) bobs: B23 and B25.

Impact of temperature on the rheological properties

The impact of temperature was investigated with a serrated bob and cup geometry (B25).

After the insertion of the NFC in the measuring chamber, the samples were allowed to reach the set temperature (5, 25 or 50°C). The samples were thereafter equilibrated for another two minutes before pre-shearing and the start of the measurements.

Impact of ionic strength on the rheological properties

The impact of ionic strength was investigated with a serrated bob and cup geometry (B25). Sodium chloride (a monovalent salt) was chosen to alter the ionic strength of the different NFC systems. The studies were conducted in the range of 0-10 mM NaCl; the samples were prepared by a method detailed in an earlier contribution (Naderi, Lindström 2014). In brief, the ≈ 2% (w/w) NFC suspensions were diluted with appropriate amounts of de-ionized water and 100 mM NaCl solutions to a total dry content of 1% ± 0.1 (w/w). The suspensions were thereafter microfluidized at 300 bar, by employing Z-

shaped interaction chambers with diameters of 400 and 200 μm, respectively.

Thixotropic properties

The samples were pre-sheared at 100 s^{-1} for one minute to even out the heterogeneities. The viscosity was subsequently recorded at $\dot{\gamma}$ = 0.1 s^{-1} over 20 min. Thereafter, the samples were sheared during 30 s at $\dot{\gamma}$ = 1000 s^{-1}, upon which the viscosity was measured again at $\dot{\gamma}$ = 0.1 s^{-1}, over 10 min. It is noted that the viscosity was sampled every second during the measurements. It is further noted that $\dot{\gamma}$ = 1000 s^{-1} lies within the range for many industrial applications (Metzger 2002).

Results and discussion

Figs 1a-c display the visual appearances of NFC_{CMC}, NFC_{Enz} and NFC_{Carb}. The NFC_{CMC} and NFC_{Enz} systems are characterized by an opaque appearance, indicating systems with a broad size distribution. NFC_{Enz} displays a coherent gel, but with a "rough" surface. However, NFC_{CMC} is characterized by a watery appearance; also, the fibrous flocs do not seem to make a coherent 3D structure. On the other hand, NFC_{Carb} is characterized by a more transparent and stiff gel structure.

Fig 1d displays the state of the fibrillated systems recorded after one week. The carboxymethylated NFC does not show any phase-separation, although phase-separation tendencies are observed for NFC_{Enz} and NFC_{CMC}. These are most visibly seen for NFC_{CMC}, where a water layer on the top of the container can be discerned.

The shear viscosity of NFC_{Enz} measured by serrated and smooth configurations (B25 and BS25) is displayed in *Fig 2a*. As evident, the shear viscosity at low shear rates ($\dot{\gamma} \leq 5$ s^{-1}) measured by the smooth geometry is lower than the viscosity measured by a serrated geometry. Furthermore, the different viscosity curves do not superimpose until high shear rates ($\dot{\gamma} \geq 50$ s^{-1}) have been reached. The kink in the viscosity curve is a common feature for many NFC systems (see e.g. Lasseuguette et al. 2008; Iotti et al. 2011; Karppinen et al. 2012; Naderi et al. 2015a). However, there are conflicting explanations for the origin of the phenomenon. For example Iotti et al. (2011) proposed the organization of the nanofibrils into "structures" to be a cause behind the observed kink in the flow curve of a low-charged NFC system. A similar explanation was also provided by Lasseuguette et al. (2008), who investigated the rheological properties of a TEMPO-based NFC. On the other hand, Karppinen et al. (2012), who combined rheological and imaging techniques (to study a presumably low-charged NFC), have argued that the kink in the flow curve is caused by the increase in the floc size and the broadening of the floc size distribution.

The rheological properties of NFC_{Enz} at 25°C, 50°C and in a 10 mM NaCl solution, measured by two serrated bobs differing in diameter (23 mm (B23) and 25 mm (B25)) are summarized in *Figs 2b-d*. Similar trends to those in *Fig 2a* are observed in all cases, i.e. differing viscosities (at low shear rates) and shifted positions of the "kink" in the flow curves. The observations indicate that rheological investigations of NFC_{Enz} are marred by slip effects. This might be related to the inherent instability of the system (*Fig 1d*). It is noted that Nechyporchuk et al. (2014) have also reported of slip effects when studying an enzymatically pre-treated NFC.

The rheological properties of NFC_{Carb} at 25°C, 50°C and in a 10 mM NaCl solution, measured by B23 and B25, and BS25 are summarized in *Fig 3*. As can be seen, the flow curves measured by B23 and B25 overlap each other, when the error margins are taken into account (see the Rheological investigations section). The results, therefore, indicate insignificant slip effects. In this context, it is noted that Nechyporchuk et al. (2014) observed no slip effects in the study of a (presumably) highly charged TEMPO-based NFC system.

The combined observations indicate that rheological measurements on stable NFC systems are little affected by slip effects, when the measurements are conducted with serrated geometries. However, the impact of wall slip effects increases with the increasing instability of the system, as is evident in Figure 2 and Figure 4; the latter displays the rheological properties of NFC_{CMC}. In this context, attention is drawn to the highly differing trends in the flow curves of NFC_{CMC} (*Fig 4*) that were obtained by B23 and B25 compared to what was observed for NFC_{Enz}, which showed similar but shifted trends. The observations in *Fig 4* correlate well with the visual appearance of NFC_{CMC} in *Fig 1*.

The rheological properties of NFC_{Enz} as a function of salt content are summarized in *Fig 5*; *Table 1* contains the stiffness (G'/G'') of the different systems. As expected, NFC_{Enz}, having a low amount of charges, is little affected by the ambient ionic strength. However, the observations contrast those of Agoda-Tandjawa et al. (2010), who reported significant increases in viscosity and G' when a (presumably) low-charged fibrillated NFC based on sugar-beet pulp was studied; the pulp contained about 1.2% (w/w) galacturonic acid. The reasons behind the discrepancy between the results of the authors and those reported in this communication are not clear. However, it is interesting to note that Agoda-Tandjawa et al. employed a plate-plate geometry with Teflon-covered surfaces (presumably with no serrations). In this context, the importance of choosing the proper geometry can also be highlighted, especially when dealing with low-charged NFC.

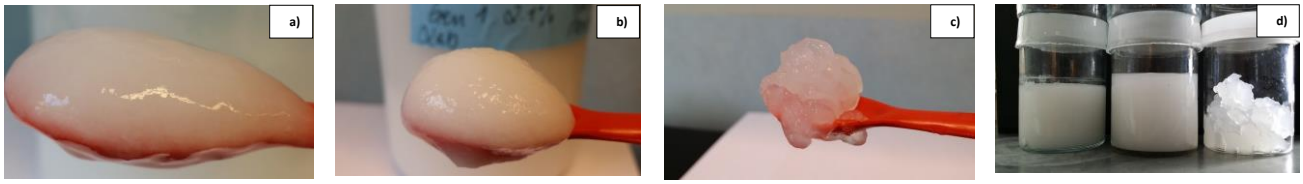

Fig 1 - The visual appearance of 2% ± 0.1 (w/w) suspensions of NFC_{CMC} (a), NFC_{Enz} (b) and NFC_{Carb} (c). d) The state of the different NFC systems recorded after one week. From left to right: NFC_{CMC}, NFC_{Enz} and NFC_{Carb}.

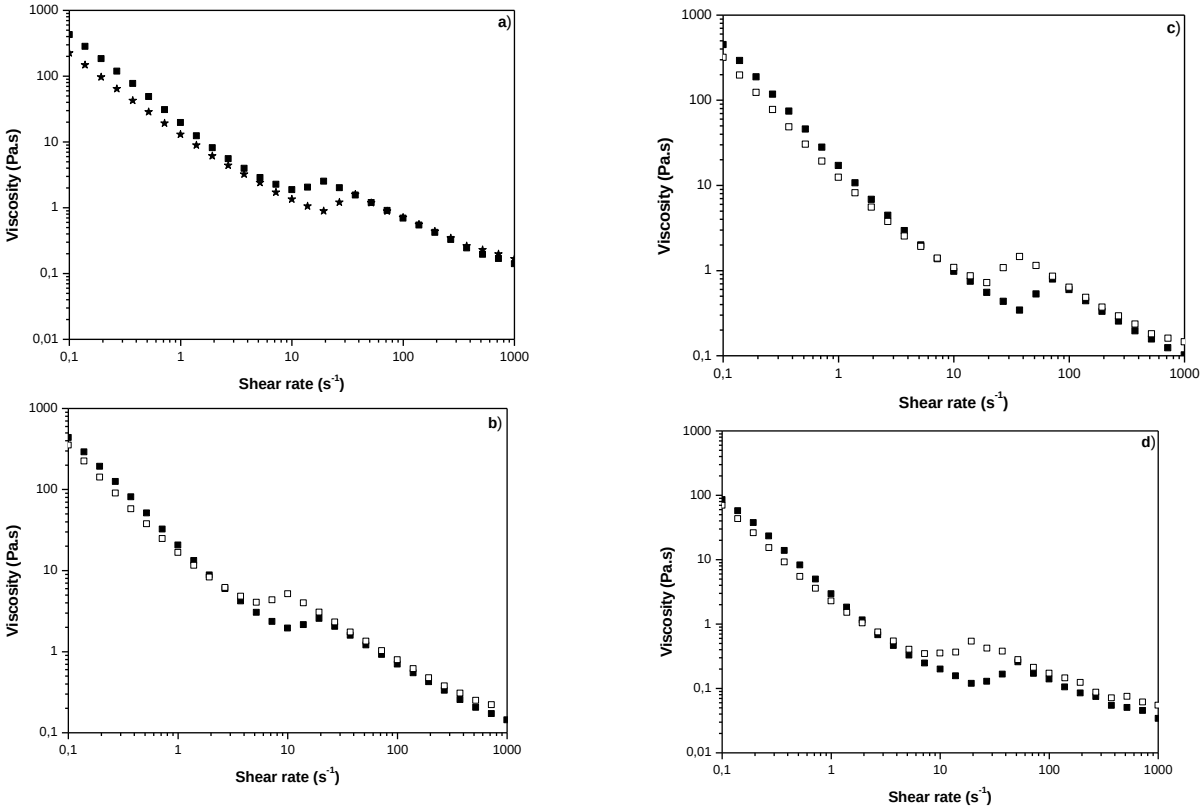

Fig 2 - Shear viscosity of NFC_{Enz} measured by different configurations. a) Serrated (square) and smooth (star) bob and cup geometries in deionized water at 25°C; B25 and BS25 were employed in the studies. Shear viscosities of NFC_{Enz} measured at 25°C b), 50°C c) and in 10 mM NaCl d). The measurements (b-d) were conducted by two different serrated bobs: B25 (filled symbol) and B23 (unfilled symbol).

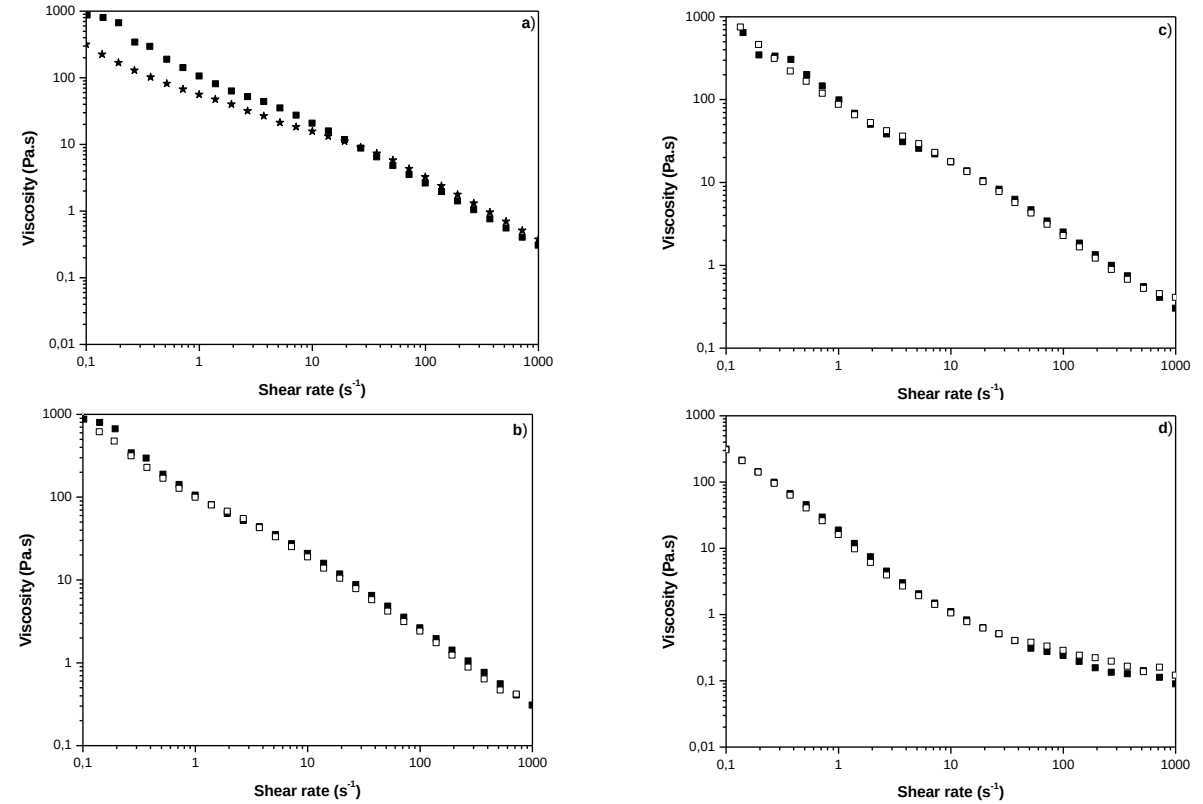

Fig - 3 Shear viscosity of NFC_{Carb} measured by different configurations. a) Serrated (square) and smooth (star) bob and cup geometries; B25 and BS25 were employed in the measurements. Shear viscosities of NFC_{Carb} measured at 25°C (b), 50°C (c) and in 10 mM NaCl (d). The measurements (b-d) were conducted by two different serrated bobs: B25 (filled symbol) and B23 (unfilled symbol).

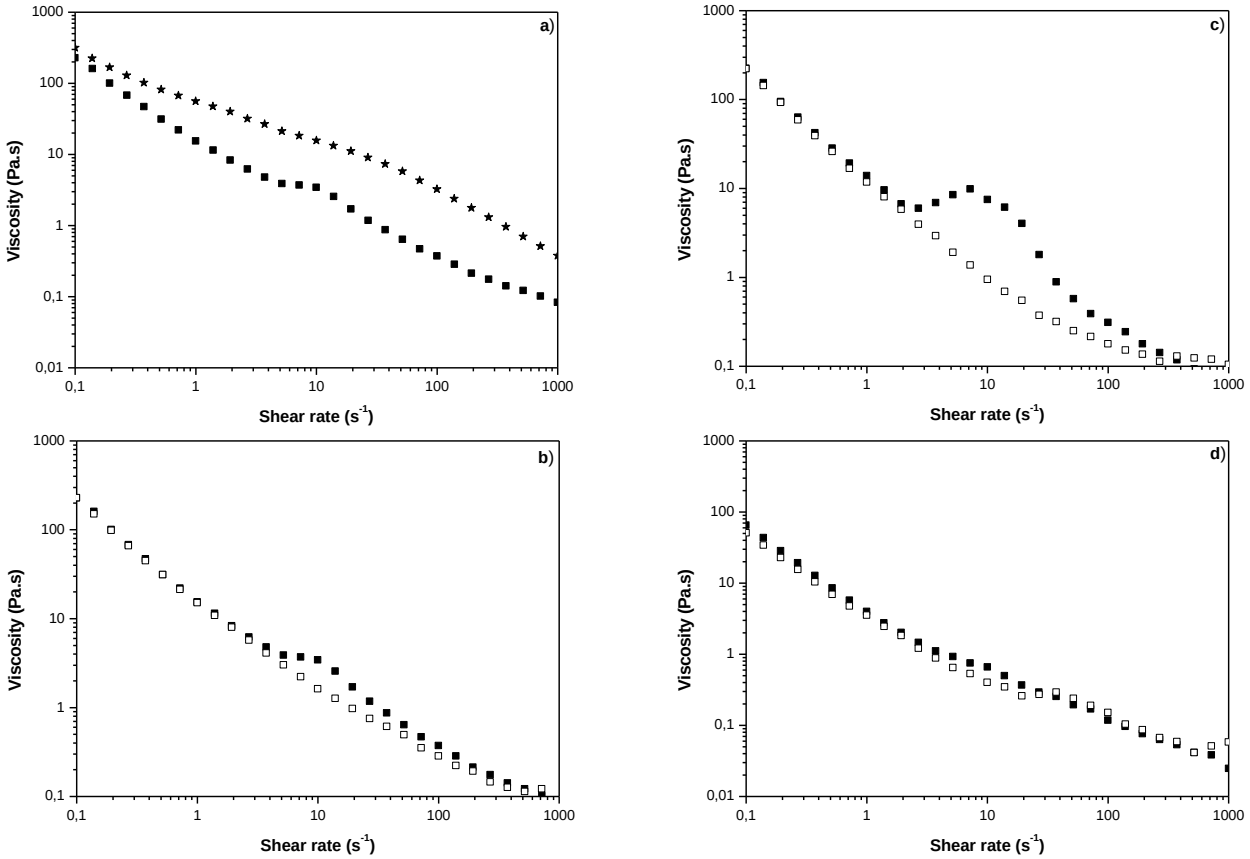

Fig - 4 Shear viscosity of NFC_{CMC} measured by different configurations. a) Serrated (square) and smooth (star) bob and cup geometries; B25 and BS25 were employed in the measurements. Shear viscosities of NFC_{CMC} measured at 25°C (b), 50°C (c) and in 10 mM NaCl (d). The measurements (b-d) were conducted by two different serrated bobs: B25 (filled symbol) and B23 (unfilled symbol).

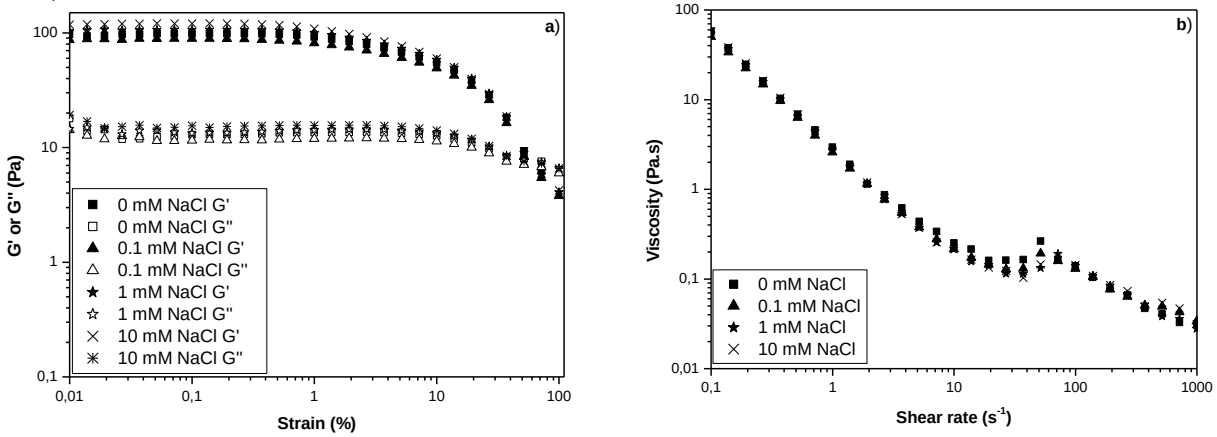

Fig - 5 Rheological properties of NFC_{Enz}, measured at about 1% (w/w) consistency, as a function of ionic strength of the system (at 25°C); B25 was employed. a) Storage (G') and loss modulus (G''). b) Shear viscosity.

For example, Naderi and Lindström (2015) showed that the water that is released upon the insertion of a NFC_{Enz} sample in a plate-plate geometry leads to the overestimation of the rheological properties, and erroneous results. This process could, however, be overcome by employing a bob and cup geometry.

Fig 6 displays the rheological properties of NFC_{CMC}; the gel stiffness of the system as a function of NaCl concentration is summarized in *Table 1*. The results in *Fig 6* imply some change in the magnitude of the rheological properties when the ionic strength is increased; this is most clearly seen in *Fig 6b*. The impact of the ionic strength is, however, more visible when the gel stiffness of the system (*Table 1*) is studied, revealing increasing stiffening when the ionic strength of the system is increased. The stiffening effect might imply a more intimate contact between the nanofibrils, but the exact mechanism behind this notion is not clear. It could be hypothesized that screening of the system charges allows for a more intimate fibril-fibril contact. However, it could also be hypothesized that increasing the ionic strength of the system further destabilizes the already unstable NFC_{CMC} system (see *Fig 1d*). Subsequently, water is released from the network, leading to the formation of a stronger network.

Table 1 - Gel stiffness (G'/G'') of different NFC system (measured at 25°C). The values for NFC_{Carb} have been reproduced from (Naderi and Lindström 2014). The storage and loss moduli for NFC_{Enz} and NFC_{CMC} were measured at γ = 0.05%. The G' and G" of NFC_{Carb} were measured at 0.5 Hz.

	G'/G''
NFC_{Enz}	
0 mM	7.9 ± 0.2
0.1 mM	7.8 ± 0.2
1 mM	7.5 ± 0.2
10 mM	8.1 ± 0.2
NFC_{CMC}	
0 mM	5.9 ± 0.2
0.1 mM	6.4 ± 0.3
1 mM	6.8 ± 0.4
10 mM	7.5 ± 1.0
NFC_{Carb}	
0 mM	11.2 ± 0.09
0.1 mM	10.4 ± 0.07
1 mM	9.7 ± 0.08
10 mM	9.1 ± 0.09

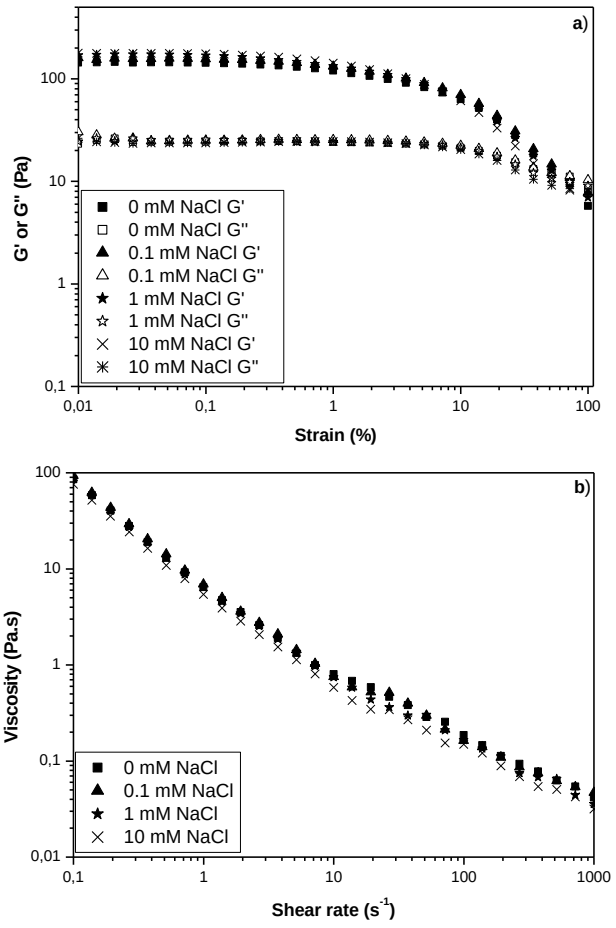

Figure - 6 Rheological properties of NFC_{CMC}, measured at about 1% (w/w) consistency (and at 25°C), as a function of ionic strength of the system; B25 was employed. a) Storage (G') and loss modulus (G''). b) Shear viscosity.

The low impact of ionic strength on the magnitude of the rheological properties (G' and viscosity) of NFC_{CMC} is puzzling, considering the higher amount of charge in the system (≈ 160 μeq/g) as compared to the charge density of NFC_{Enz} (≈ 30 μeq/g). The reasons behind this phenomenon are not understood by the authors. It may be that the amount of charge in the system is too low to have a major impact on the properties of the system. In the literature, the bulk of investigations have been conducted on highly charged NFC systems. For example, major changes in the rheology of TEMPO-based NFCs (< 2000 μeq/g) with the addition of salts have been reported by several groups (Jowkarderis, van de Ven 2014; Tanaka et al. 2014). The impact of salt on the rheology of a NFC_{Carb} system (similar to the system of this report, ≈ 590 μeq/g) has also recently been reported by the authors (Naderi, Lindström 2014); significant lowering in the viscosity and storage modulus of the system were observed already at 1 mM NaCl addition.

The stiffness of NFC_{Carb} systems as a function of ionic strength, reproduced from (Naderi, Lindström 2014), is summarized in *Table 1*. Interestingly, gel stiffness decreases with increasing ionic strength; it is recapitulated that the viscosity of the system also reportedly decreased with increasing ionic strength of the system (Naderi and Lindström 2014). The observations can be explained by the screening of the surface charges, which gives the system a more fluid-like character when water is released from the fibril-network.

The impact of temperature on the rheological properties of the different NFCs is displayed in *Fig 7*; the gel stiffness of the systems is summarized in *Table 2*. The results (*Figs 7a-b*, *Table 2*) indicate that the viscosity and G' decrease and the gel stiffness of NFC_{Enz} increases with increasing temperature. Similar effects are also observed for NFC_{CMC} (*Fig 7c-d*). However, the impact of temperature on the magnitude of the rheological properties of NFC_{Carb} is lower (*Fig 7e-f*); even though a significant increase in gel stiffness is still observed (*Table 2*).

Oscillatory measurements conducted in the linear viscoelastic regime, on NFC systems provide insight about the properties of intact systems. On the other hand, shear rate measurement provide information about flowing systems, where the networks are in the process of breaking. Hence, conflicting trends in the properties might occur when oscillatory and shear rate results are analysed.

The impact of temperature on the viscosity of nanofibrillated systems has already been studied by Herrick et al. (1983), who found that increasing the temperature (T ≤ 80°C) leads to lowering of the shear viscosity. A similar finding has also been reported by Iotti et al. (2011).

The thixotropic behaviour of the different nanofibrillated systems is presented in Figures 8a-b. The viscosity of NFC_{Carb} is rapidly restored, and most of the G' is regained quickly when the high shearing is stopped. The observations can be rationalized by using earlier discussions and considering the visual appearances of the systems. Carboxymethylated NFC is a highly fibrillated system with a strong networking ability. Hence, the viscosity of the system is rapidly regained due to the

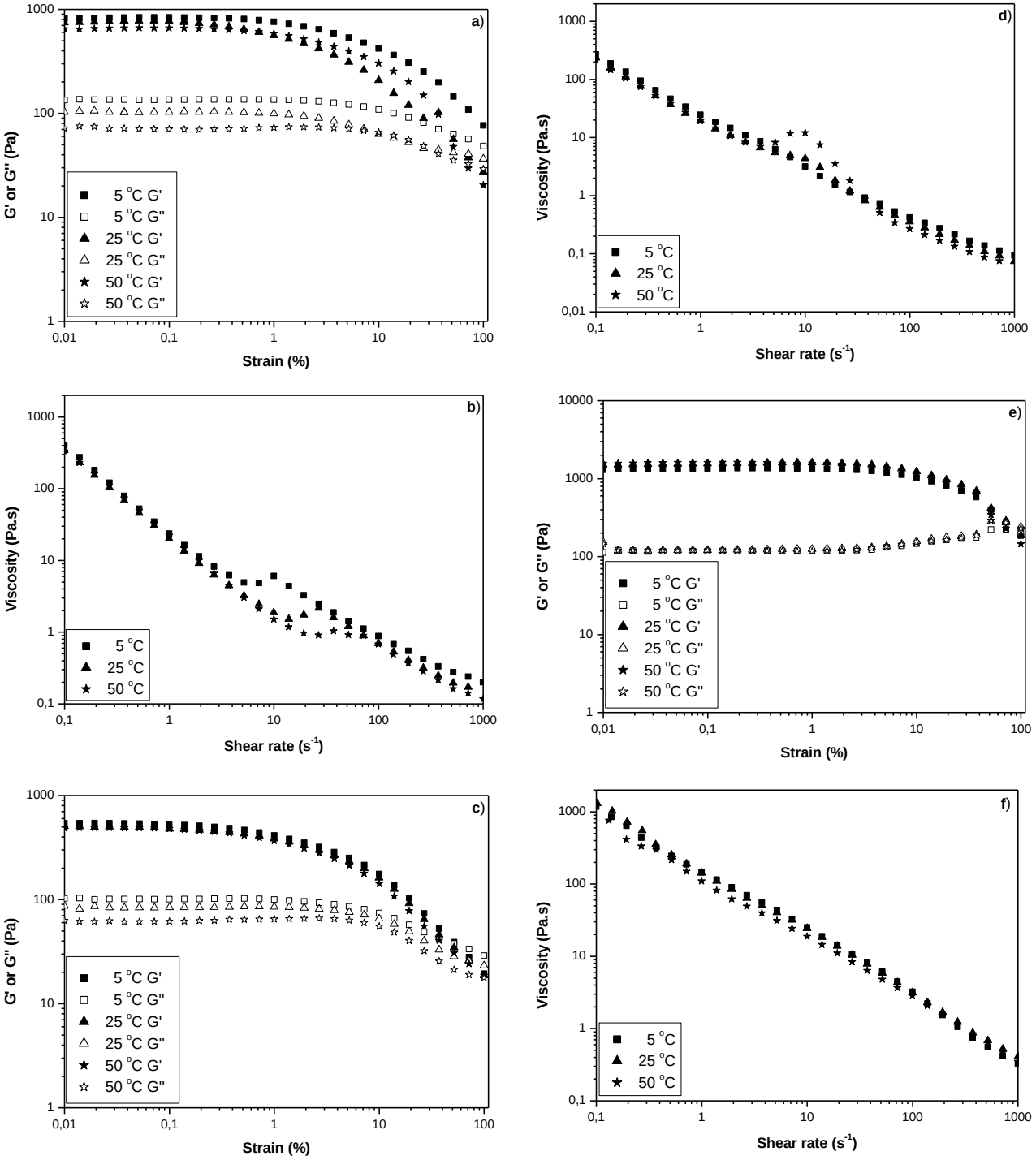

Figure - 7 Rheological properties of NFC_{Enz} (a,b), NFC_{CMC} (c,d) and NFC_{Carb} (e,f) as a function of temperature. The dry content of the different systems is 2.0 ± 0.1% (w/w). B25 was employed in the studies.

rapid networking of the system constituents. The storage modulus of the system is, however, not fully restored during the experimental time. It is postulated that prolonged times are needed for the NFC network to reach optimum strength, as noted by among others Rudraraju and Wyandt (2005).

The trends of the viscosity and G' curves of NFC_{Enz} might at first glance be challenging to rationalize, as they indicate that stronger networks are built after severe shearing of the system. However, similar observations on an NFC_{Enz} system were recently reported by the authors (Naderi et al. 2015b), in which the observations were rationalized by a more homogeneous distribution of the NFC flocs when the system was severely sheared. The severe shearing was proposed to break the larger flocs into smaller ones, which then interact more strongly with each other, due to the larger surface area of the smaller entities. This hypothesis finds support in *Fig 8c*, in which the NFC_{Enz} system has been pre-sheared for 10 min at 1000 s^{-1}. Evidently, the G' of the system after the severe shearing process is close to the G'-value that was recorded before the severe shearing process.

Table 2 - Shear viscosity and gel stiffness (G'/G'') of the different nanofibrillated systems (displayed in *Fig 7*) as a function of temperature (T). The relative changes in the magnitude of the different parameters as a function of temperature have also been included. Storage and loss modulus were measured at γ = 0.05%; shear viscosity was measured at $\dot{\gamma} \approx 700$ s^{-1}.

	Viscosity (Pa.s)	$\text{Viscosity}_T/\text{Viscosity}_{5°C}$	G'/G''	$(G'/G'')_T/(G'/G'')_{5°C}$
NFC_{Enz}				
5°C	0.24 ± 0.03	1.0 ± 0.06	6.2 ± 0.07	1.0 ± 0.01
25°C	0.17 ± 0.01	0.71 ± 0.04	7.6 ± 0.15	1.22 ± 0.02
50°C	0.12 ± 0.01	0.49 ± 0.09	9.3 ± 0.1	1.5 ± 0.01
NFC_{CMC}				
5°C	0.11 ± 0	1.0 ± 0.04	5.3 ± 0.3	1.0 ± 0.08
25°C	0.09 ± 0	0.84 ± 0.04	6.0 ± 0.05	1.13 ± 0.06
50°C	0.08 ± 0.01	0.68 ± 0.14	8.0 ± 0.4	1.51 ± 0.07
NFC_{Carb}				
5°C	0.46 ± 0.06	1 ± 0.2	11.4 ± 0.5	1.0 ± 0.06
25°C	0.51 ± 0.03	1.09 ± 0.14	12.7 ± 0.7	1.11 ± 0.07
50°C	0.47 ± 0.03	1.0 ± 0.15	13.4 ± 0.5	1.18 ± 0.05

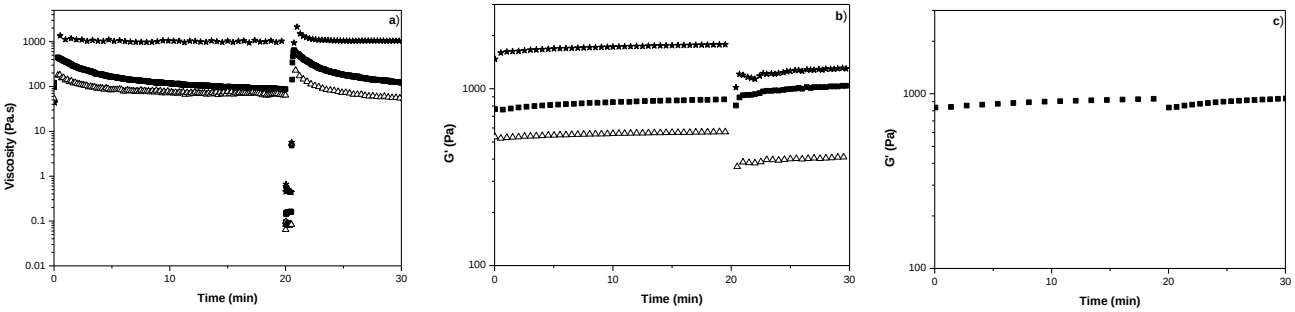

Fig - 8 Thixotropic behaviours of NFC_{Enz} (square), NFC_{CMC} (triangle), and NFC_{Carb} (star); measured at about 2% (w/w), and 25°C, and by employing B25. a) Shear viscosity. b) Storage modulus. c) The thixotropic behaviour of NFC_{Enz} that has been pre-sheared for 10 min at 1000 s^{-1}.

The thixotropic behaviour of NFC_{CMC} has elements of b**o**th NFC_{Carb} and NFC_{Enz}. The viscosity of the system can be rationalized in a similar manner as to NFC_{Enz}. The lower G'-value of NFC_{CMC}, after the severe shearing process, is postulated to be caused by the lower networking ability of the system compared to NFC_{Enz}, due to the lower fibrillated state of the former system (see *Fig 1a*).

Concluding remarks

A wide range of dispersed systems are prone to slip effects; many nanofibrillated cellulose systems belong to this category of materials. The occurrence of slip effects in NFC systems is dependent on the inherent stability of the systems, as was shown in this communication. The highly charged and highly fibrillated NFC_{Carb} was found not to be significantly affected by slip effects, but the unstable NFC_{Enz} and NFC_{CMC} displayed wall depletion effects. Interestingly, the magnitude of the slip effects in the latter systems, recorded by employing the methodology of Kelessidis et al. (2010), were found to be small. This is postulated to be due to the efficient mixing of the systems (Kelessidis et al. 2007; Bonn and Denn 2009) by the pre-shearing process of the measuring protocol. The low magnitude of the slip effects was used to draw the following conclusions on the impact of ionic strength and temperature on the rheological properties of the different NFC systems, and the thixotropic properties of the same.

It was shown that the rheological properties of NFC_{Enz} are little affected by the ionic strength of the system (at least in the investigated range). However, an increasing gel stiffening effect was observed for NFC_{CMC} with increasing ionic strength of the system; NFC_{Carb} displayed, on the other hand, an opposite trend with regard to the effect of the ionic strength of the system.

Gel stiffening effects as a function of increasing ambient temperature were observed for all systems. A lowering viscosity with increasing temperature was also observed for NFC_{Enz} and NFC_{CMC}; however, the viscosity of NFC_{Carb} was little affected by temperature.

Finally, it was found that all the investigated nanofibrillated systems could rapidly regain their original rheological properties, once their severe shearing is stopped.

The major conclusion of this work is, however, that different NFC systems can have completely different rheological properties; the awareness of this realization is important for the implementation of NFCs in the industry.

Acknowledgements

Åsa Engström and Åsa Blademo are thanked for their competent supporting work.

BillerudKorsnäs, Borregaard, Fibria, Hansol Paper, Holmen, ITC, Mercer, Stora Enso and Södra are acknowledged for their financial contribution

References

Agoda-Tandjawa, G., Durand, S., Berot, S., Blassel, C., Gaillard, C., Garnier, C. and Doublier, J. L. (2010): Rheological characterization of microfibrillated cellulose suspensions after freezing, Carbohydr. Polym. 80(3), 677-686.

Bonn, D. and Denn, M. M. (2009): Yield stress fluids slowly yield to analysis, Science (Washington, DC, U. S.) 324, 1401-1402.

Buscall, R. (2010): Letter to the Editor: Wall slip in dispersion rheometry, J. Rheol. 54(6), 1177-1183.

Henriksson, M., Henriksson, G., Berglund, L. A. and Lindström, T. (2007): An environmentally friendly method for enzyme-assisted preparation of micro-fibrillated cellulose (MFC) nanofibres, Eur. Polym. J. 43(8), 3434-3441.

Herrick, F. W., Casebier, R. L., Hamilton, J. K. and Sandberg, K. R. (1983): Microfibrillated cellulose: morphology and accessibility, J. Appl. Polym. Sci. Applied Polymer Symposium 37, 797-813.

Iotti, M., Gregersen, Ø., Moe, S. and Lenes, M. (2011): Rheological studies of microfibrillar cellulose water dispersions, J. Polym. Environ. 19(1), 137-145.

Isogai, A. (2013): Wood nanocelluloses: fundamentals and applications as new bio-based nanomaterials, J. Wood Sci. 59(6), 449-459.

Isogai, A., Saito, T. and Fukuzumi, H. (2011): TEMPO-oxidized cellulose nanofibers, Nanoscale 3(1), 71-85.

Jowkarderis, L. and van de Ven, T. G. M. (2014): Intrinsic viscosity of aqueous suspensions of cellulose nanofibrils, Cellulose 21(4), 2511-2517.

Karppinen, A., Saarinen, T., Salmela, J., Laukkanen, A., Nuopponen, M. and Seppälä, J. (2012): Flocculation of microfibrillated cellulose in shear flow, Cellulose 19(6), 1807-1819.

Katz, S., Beatson, R. P. and Scallan, A. M. (1984): The determination of strong and weak acidic groups in sulfite pulps, Sven. Papperstidn. 87, R48-R53.

Kelessidis, V. C., Hatzistamou, V. and Maglione, R. (2010): Wall slip phenomenon assessment of yield stress pseudoplastic fluids in Couette geometry, Appl. Rheol. 20(5), 52656/1-52656/8.

Kelessidis, V. C., Tsamantaki, C. and Dalamarinis, P. (2007): Effect of pH and electrolyte on the rheology of aqueous Wyoming bentonite dispersions, Appl. Clay Sci. 38, 86-96.

Laine, J., Lindström, T., Nordmark, G. G. and Risinger, G. (2000): Studies on topochemical modification of cellulosic fibers. Part 1. Chemical conditions for the attachment of carboxymethyl cellulose onto fibers, Nord. Pulp Pap. Res. J. 15, 520-526.

Lasseuguette, E., Roux, D. and Nishiyama, Y. (2008): Rheological properties of microfibrillar suspension of TEMPO-oxidized pulp, Cellulose 15(3), 425-433.

Lindström, T., Aulin, C., Naderi, A. and Ankerfors, M. (2014): Microfibrillated cellulose, Encyclopedia of Polymer Science and Technology.

Metzger, T. G. (2002): The rheology handbook: for users of rotational and oscillatory rheometers, Vincentz Curt R. Verlag.

Mohtaschemi, M., Dimic-Misic, K., Puisto, A., Korhonen, M., Maloney, T., Paltakari, J. and Alava, M. (2014): Rheological characterization of fibrillated cellulose suspensions via bucket vane viscometer, Cellulose 21(3), 1305-1312.

Moon, R. J., Martini, A., Nairn, J., Simonsen, J. and Youngblood, J. (2011): Cellulose nanomaterials review: structure, properties and nanocomposites, Chem. Soc. Rev. 40(7), 3941-3994.

Naderi, A. and Lindström, T. (2014): Carboxymethylated nanofibrillated cellulose: effect of monovalent electrolytes on the rheological properties, Cellulose 21(5), 3507-3514.

Naderi, A. and Lindström, T. (2015): Rheological measurements on nanofibrillated cellulose systems: A science in progress In: Cellulose and cellulose derivatives: synthesis, modification and applications, Monda, H. I. (ed.).

Naderi, A., Lindström, T. and Sundström, J. (2014): Carboxymethylated nanofibrillated cellulose: rheological studies, Cellulose 21(3), 1561-1571.

Naderi, A., Lindström, T. and Sundström, J. (2015a): Repeated homogenization, a route for decreasing the energy consumption in the manufacturing process of carboxy-methylated nanofibrillated cellulose?, Cellulose 22(2), 1147-1157.

Naderi, A., Lindström, T., Sundström, J. and Flodberg, G. (2015b): Can redispersible low-charged nanofibrillated cellulose be produced by the addition of carboxymethyl cellulose?, Nord. Pulp Paper Res. J. 30(4), 568-577

Naderi, A., Lindström, T., Sundström, J., Pettersson, T., Flodberg, G. and Erlandsson, J. (2015c): Microfluidized carboxymethyl cellulose modified pulp: a nanofibrillated cellulose system with some attractive properties, Cellulose 22(2), 1159-1173.

Nechyporchuk, O., Belgacem, M. and Pignon, F. (2015): Concentration effect of TEMPO-oxidized nanofibrillated cellulose aqueous suspensions on the flow instabilities and small-angle X-ray scattering structural characterization, Cellulose, 22(4), 1-14.

Nechyporchuk, O., Belgacem, M. N. and Pignon, F. (2014): Rheological properties of micro-/nanofibrillated cellulose suspensions: Wall-slip and shear banding phenomena, Carbohydr. Polym. 112, 432-439.

Rudraraju, V. S. and Wyandt, C. M. (2005): Rheological characterization of Microcrystalline Cellulose/Sodium carboxy-methyl cellulose hydrogels using a controlled stress rheometer: part I, Int. J. Pharm. 292(1-2), 53-61.

Tanaka, R., Saito, T., Ishii, D. and Isogai, A. (2014): Determination of nanocellulose fibril length by shear viscosity measurement, Cellulose 21(3), 1581-1589.

Walecka, J. A. (1956): An investigation of low degree of substitution carboxymethylcellulose, Tappi J. 39(7), 458-463.

Wågberg, L., Decher, G., Norgren, M., Lindström, T., Ankerfors, M. and Axnaes, K. (2008): The build-up of polyelectrolyte multilayers of microfibrillated cellulose and cationic polyelectrolytes, Langmuir 24(3), 784-795.

Manuscript received February 19, 2016
Accepted May 4, 2016